Development of a dynamic *in vitro* stretch model of the alveolar interface with aerosol delivery

Daniele Cei[1,2,3,i], Ali Doryab[3,4,i], Anke-Gabriele Lenz[3,4], Andreas Schröppel[3,4], Paula Mayer[3,4], Gerald Burgstaller[3,4], Roberta Nossa[1,2], Arti Ahluwalia[1, 2,i], Otmar Schmid[3,4,i]

[1] Research Center "E. Piaggio", University of Pisa, Largo Lucio Lazzarino 2, 56126 Pisa, Italy

[2] Department of Information Engineering, University of Pisa, via Caruso 2, 56126 Pisa, Italy

[3] Comprehensive Pneumology Center, Member of the German Center for Lung Research (DZL), Max-Lebsche-Platz 31, 81377 Munich, Germany

[4] Institute of Lung Biology and Disease, Helmholtz Zentrum Muenchen, Ingolstaedter Landstrasse 1, D-85764 Neuherberg, Germany

We describe the engineering design, computational modelling and empirical performance of a Moving Air-Liquid Interface (MALI) bioreactor for the study of aerosol deposition on cells cultured on an elastic, porous membrane which mimics both air-liquid interface exposure conditions and mechanoelastic motion of lung tissue during breathing. The device consists of two chambers separated by a cell layer cultured on a porous, flexible membrane. The lower (basolateral) chamber is perfused with cell culture medium simulating blood circulation. The upper (apical) chamber representing the air compartment of the lung is interfaced to an aerosol generator and a pressure actuation system. By cycling the pressure in the apical chamber between 0 and 7 kPa, the membrane can mimic the periodic mechanical strain of the alveolar wall. Focusing on the engineering aspects of the system, we show that membrane strain can be monitored by measuring changes in pressure resulting from the movement of media in the basolateral chamber. Moreover, liquid aerosol deposition at a high dose delivery rate (>1 µl cm^{-2} min^{-1}) is highly efficient (ca. 51.5%) and can be accurately modelled using finite element methods. Finally, we show that lung epithelial cells can be mechanically stimulated under air-liquid interface and stretch-conditions without loss of viability. The MALI bioreactor could be used to study the effects of aerosol on alveolar cells cultured at the air-liquid interface in a biodynamic environment or for toxicological or therapeutic applications.

Keywords— Bioreactor, Air-Liquid Interface, Aerosol exposure, Flexing Membrane.

1. Introduction

During the past decade, the development of bioreactors and microfluidic systems (organ-on-chip) for organotypic *in vitro* models has been a dynamic field of research with the vision of reducing or even replacing *in vivo* animal studies in drug development and risk assessment. One of the keys to success is the establishment of biomimetic culture and exposure conditions, which is expected to enhance the capacity of *in vitro* models to predict outcomes for human health.

The lung is one of the most challenging organs for *in vitro* modelling since it is not only perfused by blood, but also in direct contact with ambient air. Inhalation of gaseous toxins, viruses and dispersed particles (aerosols) may cause inflammation and stress, contributing to the development or exacerbation of diseases such as asthma or chronic obstructive pulmonary disease (Hänninen et al., 2010; Peters et al., 1997). The smallest, ultrafine or nano-sized particles (less than 100 – 300 nm in diameter) are especially under intense scrutiny due to their enhanced surface area (per unit mass), which has been associated with the prevalence of acute and chronic lung disease (Peters et al., 1997; Schmid and Stoeger, 2017), and their enhanced probability of translocation from the lung to blood circulation and from there to almost all secondary organs such as liver, brain and even placenta (Kreyling et al., 2013). On the other hand, inhalation of medical aerosol has a long-standing history in the treatment of lung diseases (Stein and Thiel, 2017).

Upon deposition of the aerosol onto the lung epithelium, the soluble fraction of the aerosol is quickly diluted by bodily fluids, while the non-soluble particles remain on the epithelium. The subsequent interaction of (non-soluble) particles with the pulmonary epithelium is a complex process, mediated by the breathing-induced rhythmical contraction of the diaphragm, which generates a periodic change in alveolar volume accompanied by stretching and relaxation of the alveolar walls. How this movement contributes to biokinetics and cellular uptake of particles within and beyond the alveolar tissue, or to downstream inflammatory processes is not clearly

understood,

partly because of the lack of appropriate models which can recapitulate the dynamic alveolar microenvironment (Min et al., 2013; Roan and Waters, 2011).

In vivo studies on the effects of inhaled aerosols are traditionally performed on animal models (Nahar et al., 2013; Sakagami, 2006). While animal models capture the general effects on peripheral tissue, the whole lung, and the entire organism, biomimetic *in vitro* testing with human cells accounts for human-specific responses to stimuli and in-depth analysis of cell/tissue-specific response pathways.

However, the predictive power of *in vitro* test systems for clinical conditions in humans is expected to depend on their biomimetic qualities, i.e. their ability to adequately model the most biologically relevant features of the *in vivo* conditions (Darquenne et al., 2016). To this end several alternative methods for mimicking the lung epithelial barrier have been developed. Perhaps the best known is the air-liquid interface (ALI) barrier model, based on a static culture of lung-derived cells grown on a permeable membrane with the apical side of the cells in contact with air and the basolateral side is wetted by medium. ALI pulmonary epithelial cells polarize, i.e. the air-side is structured differently than the medium side resembling the *in vivo* conditions in various aspects including cilia-formation, formation of tight cell-cell contacts as well as secretin of lung lining fluid (Paur et al., 2011). Nevertheless, growing pulmonary cells on a static membrane at the ALI does not mimic the periodic mechanical strain experienced by alveolar cells under *in vivo* conditions due to breathing, which may affect the cellular response to toxins or therapeutics (Cavanaugh et al., 2006; Min et al., 2013; Savla et al., 1997; Schmekel et al., 1992).

ALI cultures also allow for direct deposition of aerosols onto epithelial cells mimicking the humid pulmonary environment *in vivo*. The currently available technologies for aerosol-cell deposition can be classified according to their employed deposition mechanisms (Paur et al., 2011), namely

diffusion and/or sedimentation (Bitterle et al., 2006), impaction (Schreier et al., 1998), electrostatic precipitation (Savi et al., 2008), thermophoretic deposition (Broßell et al., 2013), gravitational settling (Hein et al., 2010) and cloud motion (Lenz et al., 2014). Although many of these devices (except for thermophoretic deposition), are commercially available, to the best of our knowledge no aerosol delivery system has yet been reported for studies on cell systems encountering cyclic stretch (Doryab et al., 2019), which has been shown to substantially alter cell physiology in terms of secretion of alveolar surfactant, metabolic activity and cytotoxicity for human alveolar epithelial cells (Huh et al., 2010). To address the issue of cyclic stretch, more advanced *in vitro* cell models have been developed and have been systematically reviewed by Doryab et al (Doryab et al., 2019). Most devices apply pneumatic or motor-driven cyclic stretch in liquid-liquid conditions (Campillo et al., 2016). The FlexCell Culture System® (Flexcell International Corp., USA) is one such commercial device with a mechanically active substrate: epithelial cells are cultured on a silicone membrane and stretched by applying negative differential pressure on the other side of the membrane. However, due to the mechanism of actuation the membrane cannot be porous and thus cannot provide ALI conditions. A number of ALI systems have been developed such as the well-based system with moving walls reported by Choe et al. (Choe et al., 2006; Tomei et al., 2008), but they do not allow for fluid flow or aerosol deposition. One of the most cited cell-stretch models is the micro-scaled lung-on-a-chip developed by the WYSS institute combines ALI conditions, and a stretchable silicone membrane and medium flow (Huh et al., 2010). The two-channel system also employs negative pressure actuation, but in a different configuration than the FlexCell device: the rectangular membrane is attached to a flexible frame on the two shorter sides. Upon mechanical activation of the frame by the application of a vacuum, the membrane stretches. Stucki *et al.* (Stucki et al., 2015) reported a lung on a chip system with a two-chamber configuration separated by a flexible membrane; the basal chamber also has a flexible bottom

which is actuated by the application of pressure. Both of these chip devices allow for perforation of the membrane and hence for ALI cell culture conditions but neither are amenable to effective and reproducible aerosol-cell delivery which are necessary for quantitative aerosol dose-cell response studies. Moreover, the handling of the peripheral microfluidic technology for maintenance of adequate cell culture conditions can be a challenge which is acknowledged by researchers developing lung-on-a-chip devices (Artzy-Schnirman et al., 2019; Doryab et al., 2016; Ehrmann et al., 2020).

Here we report the engineering of a Moving Air Liquid Interface (MALI), bioreactor as an enabling tool for studies on pulmonary cells and tissues in physiological and pathological conditions. The bioreactor consists of an apical and basolateral compartment separated by a pressure actuated flexible membrane. Designed on the scale of a standard 6-well Transwell, the bioreactor's basolateral compartment contains cell culture medium, which flows through the bioreactor mimicking blood circulation while the apical side is interfaced with a nebulizer for efficient, dose-controlled aerosol delivery to cells. MALI's performance was investigated in terms of cyclic membrane stretch and aerosol delivery characteristics. An evaluation of the cytocompatibility of the system components was performed assessing the effect of physiologic cyclic stretch on A549 lung epithelial cells.

2. Design of the MALI system

2. 1. Overall design and working principle

At the heart of the MALI system is the modular MALI bioreactor, similar to that described in Mazzei *et al.* (Mazzei et al., 2010) and Giusti *et al.* (Giusti et al., 2013). The bioreactor with its two chambers and their respective hydraulic and pneumatic circuits is depicted in Figure 1A. Between the two chambers is a flexible porous membrane for cell culture which mimics the alveolar air-tissue interface. A peristaltic pump drives medium through the basolateral chamber modelling the

blood side and providing a continuous nutrient supply to the cell layer as well as removal of metabolites and signalling molecules which may also be delivered to other bioreactors with cells or tissues from other organs (e.g. liver). The apical chamber simulates the air-facing side of the alveolar barrier and includes a pair of electropneumatic regulators and a clinically relevant aerosol generator. The latter provides dose-controlled aerosolized substance delivery to the cells simulating drug delivery during inhalation therapy or exposure to airborne particles.

The membrane is actuated by cyclic switching of two pressure regulators, which allow oscillation of air pressure in the apical chamber between ambient and a few kPa above ambient pressure. This in turn leads to a periodic downward deflection and relaxation of the membrane simulating the inhalation and exhalation phase during respiration. Figure 1B shows the complete MALI system which is described in detail herein. The system was designed to recapitulate the cyclic stretch of the alveoli during breathing, covering both physiological and pathological levels of strain (physiological: 4-12% linear strain[ii], pathological up to 20% linear strain) at a typical breathing frequency of 0.2 Hz (Huh et al., 2010; Patel, 2011; Ren et al., 2009; Roan and Waters, 2011; Vlahakis et al., 1999; Waters et al., 2012).

2.2. FEM modeling of the MALI bioreactor

The MALI bioreactor's design and performance were simulated using finite element methods (FEM). A first model of the basolateral chamber was used to optimise its dimensions by evaluating the displacement field of the membrane at different bioreactor heights and different pressures applied apically to the elastic membrane (described in Section 3). A second FEM model was used to estimate the deposition of aerosol on the membrane in the apical chamber both in terms of total dose and spatial distribution.

2.3. FEM model of the basolateral chamber including membrane activation

The basolateral chamber model was generated using the fluid structure interaction (FSI) module of the Comsol Multiphysics 4.3a software (COMSOL AB, Stockholm, Sweden). The domain consists of a cylindrical chamber with variable height and an inlet and outlet for cell culture media (Fig. S1), while the membrane is modelled as a deformable disk (with the same elastic modulus as the membrane used for cell culture, see Section 3) placed on top of the basolateral chamber of the bioreactor and subject to a variable positive pressure from the top simulating air pressure in the apical chamber. A sequence of quasi-static conditions, is used to simulate the stretching motion of the membrane. In particular, the steady state condition for constant apical pressure is modelled for a range of pressures covering that applied during dynamic activation of the membrane. Viscous drag and fluid pressure on the membrane resulting from the flow of medium is also accounted for. The fluid dynamics was solved in the laminar flow regime for an inflow of 0.4 mL min^{-1} as suggested by Mazzei *et al.* (Mazzei et al., 2010). No slip conditions were assumed at all interfaces including the virtual wall representing the membrane, which was also coupled with the FSI module to account for its displacement.

The model was solved for different bioreactor heights (H = 10-20 mm, 1 mm increments) and various apical differential pressures across the membrane (1 to 10 kPa, 1 kPa increments). The optimum height is the best compromise between a small chamber volume (i.e. low height, yet sufficient to allow obstruction-free membrane stretching) and low applied pressure to achieve a given membrane deformation. In fact, the larger the chamber, the lower the flow resistance when medium is squeezed out of the chamber by membrane motion. To simulate pathological strains (20%), the maximum vertical displacement of the centre of the membrane in the z-direction required during operation was estimated as ≈7 mm. A total chamber height of 14 mm was considered the best compromise to allow unencumbered displacement of the membrane with low

pressure values (maximum 7 kPa in the model) while maintaining a chamber with a volume reasonably close to that of a typical cell culture well. An example of membrane displacement is shown in Figure 2A, while videos of the model can be downloaded from the Supplementary Information (SI).

2.4. FEM modelling of the apical chamber including aerosol deposition

To guarantee dose-controlled aerosol delivery, we based the dimensions of the apical chamber on that of the ALICE cloud device reported in Lenz *et al.* (Lenz et al., 2009). The patented technology takes advantage of the generation of a cloud which is more efficient for aerosol deposition onto cells in ALI conditions with respect to single droplet dynamics. The main technical refinement of the aerosol unit of the MALI bioreactor relates to the use of a cylindrical aerosol exposure chamber with a cross-sectional area just large enough to expose the ca. 5 cm^2 membrane in the bioreactor as compared to the relatively large cubical exposure chamber of the ALICE Cloud system (ca. 125 cm^2), which was designed for simultaneous exposure of up to six 6-well transwell inserts (Lenz et al., 2014). The FEM model of the apical chamber was developed to evaluate aerosol cloud deposition on the membrane. As the geometry is axially symmetric (Figure 2B) it was solved with a 2D model.

Typically, the nebulizer is filled with 10 µL of an aqueous solution. It emits a dense cloud of aerosol with a speed of about 2.5 m/s directly into the aerosol inlet tube which leads into the apical chamber (Figure 2B). Using the computational fluid dynamics software Fluent 14.0 (Ansys Inc., Pennsylvania, USA), cloud motion in the air-filled chamber was modelled with the Eulerian Multiphase module (here two phases: air and cloud), where the dense cloud (i.e. droplet suspension) is treated as a secondary fluid interacting with the primary fluid (air). Each fluid phase was solved with the Eulerian discretization method and their interaction was taken into account

assuming no slip at the boundaries of the domain. Input parameters for the model are reported in the SI.

As the Eulerian-Eulerian method is not able to evaluate particle deposition onto surfaces due to the two-phase approach taken, an Eulerian Wall Film module was added to the model. Here, the interaction between fluid phase and wall surface is considered in order to evaluate film formation due to particle settling. Continuity and momentum equations were modified in order to evaluate deposition effects due to liquid-wall collision under the influence of inertial impaction and gravitational settling. A User Defined Function (UDF) was compiled to simulate accumulation of liquid on the bottom of the apical chamber where the membrane is located. The UDF generates a negative source term (sink) extracting the part of the fluid that collides with the membrane and considers it as "collected" from the liquid phase.

As seen from Figure 2C and the videos (SI), the modelled cloud velocity profile at the beginning of the aerosol exposure (0.4 s after activation of the nebulizer) propagates through the centre of the tube and deposits at the base and sides of the apical chamber. Figure 2D depicts the spatial uniformity of the aerosol deposited on the membrane at the end of the exposure. The result indicates uniform aerosol deposition over the entire cell-covered area except for a narrow region at the rim. An analysis of the deposition efficiency reveals that 85% (asymptotic value) of the liquid settles on the membrane within 5 minutes.

3. Materials and Experimental Methods

The design, construction and testing of the main components of the MALI system are described here, with further technical details reported in the SI.

3.1. Membrane fabrication and characterization

Electrospun Bionate® II 80A (The Electrospinning Company, Oxfordshire, UK) was used as a flexing membrane and porous support for epithelial cells. Bionate® is a biocompatible poly(carbonate)urethane copolymer used in chronically implanted devices (i.e. pacemaker leads, ventricular assist devices, catheters, hip/knee joints etc. (Bélanger et al., 2000; Khan et al., 2005; Zdrahala and Zdrahala, 1999). According to the manufacturer's specifications, the membranes are 75.4±6.6 µm thick (Lehmann et al., 2011b), with a fibre diameter of 3.06± 0.36 µm. These parameters are consistent with our measurements from confocal microscopy.

The mechanical properties of the Bionate® membranes were evaluated for assessing their suitability as a stretchable support for alveolar cell culture systems. First, the elastic modulus was evaluated using a twin column testing machine (Z005, Zwick-Roell, Germany) equipped with a high precision load cell (loading 10 N, resolution 20 mN) under dry conditions, with a uniaxial strain rate of 0.1% s^{-1}. Rectangular samples were stretched up to 30% of their initial length in order determine the extent of the elastic region. The Bionate® membrane was also soaked for 0, 1, 2, 4, and 7 days in culture media (DMEM, see section 3E and SI) at 37°C and the mechanical tests were repeated for evaluation of fatigue effects while submerged in DMEM at 37°C. In addition, cyclic deformation was applied for 3h at a strain corresponding to normal breathing conditions (5% strain, 0.2Hz, 37°C in DMEM). The elastic modulus was evaluated at different time points (1, 2, 4 and 24h) through least squares linear fitting of the uniaxial stress-strain curve.

3.2. Fabrication of MALI bioreactor

Both chambers of the MALI bioreactor are fabricated from polydimethylsiloxane (PDMS, Sylgard 184 kit, Mascherpa, Milano, Italy), using milli-molding as described in Vozzi *et al.* (Vozzi et al., 2011). The Bionate® membrane is clamped between two 3D printed polylactide acid (PLA) rings designed with a press-and-click male-female coupling as shown in Figure S3C (SI). Once assembled

in the ring, the membrane can be easily handled without touching or damaging. The PLA ring with the membrane is lodged in a PDMS hoop and inserted between the apical and basolateral chambers (see SI, Fig. S3B).

3.3. Fluidic system and membrane displacement

The basolateral chamber is perfused with media through a peristaltic pump and a fluid reservoir. When a positive pressure is applied in the apical chamber, the actuation of the membrane results in displacement of some of the basolateral medium into the media reservoir (Figure 1A). As the reservoir is air tight, any change in medium volume will result in a change of air pressure in the vessel, which is directly related to the displaced medium volume according to the general gas law or by performing a simple pressure-volume calibration. Assuming that no liquid passes through the membrane (which is the case here) and that the membrane actuation results in a hemispherical deformation of the membrane, the displaced medium volume can be related to the linear strain exerted on the deformed membrane through classical equations of thin shell mechanics (See SI). Hence, by monitoring the differential air pressure in the medium reservoir during the application of cyclic over pressure in the apical chamber, the membrane strain can be monitored in real-time. Further details on the components of the fluidic and control system are reported in the SI.

3.4. Aerosol delivery system and aerosol dosimetry

The apical compartment consists of three parts (Fig. 1 and 2A): The cylindrical apical chamber, a vibrating mesh nebulizer (Aeroneb Pro/Lab, Aerogen Inc., Galaway Ireland) positioned axially above the stretchable membrane and a cylindrical aerosol tube connecting both elements (Barapatre et al., 2015; Lenz et al., 2014). Membrane actuation is interrupted during operation of the nebulizer and subsequent aerosol settling, which typically takes less than a couple of minutes (for 10 µL of nebulized liquid).

Measurements of aerosol dose and distribution on the membrane were performed with quantitative spectrophotometry and a fluorescence imaging system, respectively (Barapatre et al., 2015; Lenz et al., 2014). For dosimetry analysis, the nebulizer was loaded with 10 µL of a 15 µg/mL fluorescein sodium salt solution in phosphate buffered saline (PBS, Sigma-Aldrich Chemie GmbH, Munich, Germany) and attached to MALI bioreactor, replacing the membrane with a glass slide to facilitate retrieval of the deposited fluorescein. After the experiment, the glass slide was carefully rinsed with 500 µl water and the fluorescein concentration in the retrieved solution was measured using a microplate fluorescence reader (Safire II, Tecan Inc., Mannedorf, Switzerland; excitation/emission = 483 nm/525 nm). The aerosol delivery efficiency was determined by normalizing the measured dose to the amount of liquid nebulized. Using this technique, the retrieval efficiency was determined to be 100% (within experimental uncertainties; data not shown).

For assessment of spatial uniformity of aerosol deposition on the cells, 10 µL of an aqueous suspension (0.05% w/v) of fluorescent polystyrene nanoparticles (SkyBlue, Kisker Biotech GmbH & CoKG, Steinfurt, Germany; particle diameter: 450 nm, excitation/emission = 680nm/720nm) was nebulized in MALI. Again, nanoparticles were deposited on a glass slide located at the position of the membrane and the resulting fluorescence pattern on the glass slides was measured with a fluorescence imaging system (IVIS Lumina II, PerkinElmer, USA).

Both sets of experiments (deposition efficiency and spatial uniformity of deposition) were performed at five different nebuliser duty cycles (100, 50, 25, 12.5 and 6%), corresponding to a range between 500 ms (100%) and 30 ms (6%) of nebulizer on-time per 500 ms time period. We note that SkyBlue nanoparticles cannot be used for determination of aerosol delivery efficiency since their retrieval efficiency from the glass slide is less than 100%. On the other hand, fluorescein cannot be used for measuring spatial uniformity of aerosol delivery onto the

membrane (glass slide) due to rapid drying of the aerosol droplets after deposition which results in quenching of the fluorescence signal. Hence, two different fluorescent tracers had to be employed for determination of both efficiency (dose) and spatial uniformity of aerosols delivered to the cells.

3.5. Cell culture

An alveolar epithelial type II-like cell line derived from a human adenocarcinoma (A549) was used to assess the impact of handling and set up of the MALI bioreactor on cells, in terms of cytocompatibility, viability and confluency of the cell layer. These cells are widely employed as a model of the alveolar epithelial barrier (Lehmann et al., 2011a; Lenz et al., 2009; Lenz et al., 2013; Oostingh et al., 2008; Ren et al., 2009; Schmid et al., 2017). We used a standard DMEM based medium, with source and components reported in the SI.

Bronchial epithelial 16HBE14o− cells (cell seeding density: 2 x10^5 cells cm^{-2}) were also used to study the cell adherence to the electrospun Bionate® membrane. Cells were cultured in MEM medium (Gibco) supplemented with 10% FCS (Gibco), 1% (v/v) Pen/Strep (100 U mL^{-1}, Gibco) for 6 days under submerged culture conditions and 2 days under ALI culture.

3.6. Preparation Bionate® membranes and cell culture

The Bionate® membranes were hydrophobic (water contact angle > 90°) and not cell adhesive in their pristine state. Thus, as detailed in the SI, they were treated with ethanol and Matrigel, which contains components present in the alveolar basal lamina. The Matrigel coated membranes were mounted in the hoops and placed in 50 mm diameter Petri dishes; 1×10^6 cells were seeded on the apical (top) side of the membrane (0.2×10^6 cells/cm²). A number of different conditions were examined to assess the impact of the various preparation and handling steps:

I. “Membrane control” (negative control) – cells were grown on the Bionate® membrane

(mounted in the PLA ring) under optimum growth conditions, i.e. cells in submerged culture conditions applying 2 mL of cell culture medium on the apical side and 8 mL in the petri dish (basolateral side) and in an incubator (5% CO_2, 37°C, 100% humidity) for the entire experimental time (7 days)

II. "Bioreactor control" – same as membrane control, but after day 6 the mounted membranes were transferred into the bioreactor prefilled with medium in the lower (basolateral) chamber and left for a further day in the incubator with no medium on the apical side.

III. "MALI non-stretched" and "MALI stretched" – same as "Bioreactor control", but, after 21h of ALI, cells were exposed to a flow (0.4 mL min^{-1}) and flow and stretch (5% strain, 0.2 Hz with perfusion rate of 0.4 mL min^{-1}) conditions, respectively for 3h.

The assessment was based on cell viability (protein content), cytotoxicity and confluency of the epithelial cell layer.

3.7. Cell assays and imaging

Cytotoxicity was assessed by detection of the enzyme lactate dehydrogenase (LDH) in the supernatant of the cell culture (LDH; Roche Applied Science, Mannheim, Germany). Leakage of LDH from the cytoplasm into the supernatant is characteristic of membrane damage.

Total protein content of cells is an indirect measure of the number of cells populating the membrane and hence of their growth and viability. It was determined from the protein concentration of the cells using the Bio-Rad Protein assay (Bio-Rad, Cat.No 500-0006, Muenchen, Germany) according to the manufacturer's protocol.

Confocal microscopy analysis allows for visualization of the cell layer on the membrane, providing information on the degree of confluency of the cell layer, their morphology and their viability status. To this end, a series of z-stack images were acquired and processed using a Carl Zeiss

LSM710 system and associated software. Scanning Electron Microscopy (SEM, Zeiss Crossbeam 340, Carl Zeiss AG, Oberkochen, Germany; operating voltage of 2 kV) was used to evaluate cell attachment of bronchial epithelial 16HBE14o− cells on the Bionate® membrane. Additional technical details on cell assays are given in the SI.

3.8. Data Analysis

Unless stated otherwise, all data are reported as mean ± standard deviation for at least three independent measurements ($n \geq 3$). The One-way ANOVA-test was used to evaluate the statistical significance of effects. Significance level was set at $p < 0.05$ for each test.

4. Results

4.1. Membrane elasticity and real-time monitoring of cyclic strain

The (uniaxial) stress-strain behaviour of the Bionate® membrane is depicted in Figure 3A. An approximately linear elastic behaviour was observed up to about 15% uniaxial strain, with an elastic modulus of 2.14 ±0.18 MPa as derived from a linear least square fit of the stress-strain curve. The elastic modulus obtained for the Bionate® membrane was not affected by incubation in DMEM at 37°C, even after seven days of complete submersion. Moreover, cyclic stretching for uniaxial strains between 1 and 15% for up to 3h under wet conditions did not alter its elastic modulus, suggesting its suitability for operation in dynamic conditions in a cell culture environment.

By measuring the change in pressure and hence volume in the mixing chamber during the application of cyclic overpressure in the apical chamber, we were able to estimate the linear strain of the membrane. As seen from Figure 3B, in the range 0 to 6 kPa overpressure, the response is

approximately linear. Moreover, the MALI bioreactor was found to be leak-tight for medium flow rates up to 1 mL min^{-1} and apical differential air pressures up to 20 kPa.

It is noteworthy, that membrane activation at a physiologic linear strain of 5% requires application of about 2 -3 kPa on the apical side (Figure 3B), slightly larger than differential pressure occurring during physiological breathing (for rest and heavy exercise conditions about 0.3 kPa and 0.9 kPa, respectively (Ravikrishnan, 2006)). However, since cells consist mainly of water and water is incompressible, they can easily cope with these small increases in pressure conditions as evidenced by our cell culture data presented in section 4C.

4.2. Aerosol Delivery

As seen from Figure 4A, we found that the delivery efficiency is 51.5±1.0% of the 10 µL of liquid filled into the nebulizer independent of the duty cycle. The aerosol was nebulized within a few seconds and subsequent cloud settling onto the cells took 1-2 minutes. We estimated the dose delivery rate to be higher than 1 µl cm^{-2} min^{-1}. After nebulization 12.6±0.4% of the invested liquid remained in the nebulizer reservoir, again without any statistically significant dependence on the duty cycle. The rest of ca. 35% must have been deposited on the lateral and top walls of the bioreactor.

Moreover, the aerosol is deposited uniformly as seen from Figure 4B, which depicts the measured fluorescence intensity on apical surface after nebulization of fluorescent aerosol. The pixel-by-pixel fluorescence (dose) variability resolved on a cellular scale (pixel: 5 µm x 5 µm) across the centreline of the membrane is 19% (9.4%/49.2%). This indicates that aerosol deposition on the cells is somewhat less uniform than predicted by the computational model (ca. 10%; see Figure 2C), which may be due to the larger grid size in the FEM model (200 µm x 200 µm). Within 0.12 cm of the wall there is a steep decrease in dose due to edge effects, as predicted by the model.

4.3. Cell viability, cytotoxicity and stretch experiments

Figure 5 indicates that handling of the cells in the MALI system does not have any detrimental effect on cell viability and cytotoxicity levels (necrosis). For all investigated cases, the protein content of the cells is constant at about 450 µg and the cytotoxicity of 4-6% is well below 10%, which is typically considered as non-toxic regime. Moreover, none of the investigated conditions differs significantly from the "Membrane control".

Confluency of the cell layer was investigated with confocal microscopy after staining for cell nuclei and actin filaments of the cytoskeleton. Figure 6 shows that cells reach confluency by the end of the day 7. While there is reasonably good cell coverage over most of the membrane (Figure. 7A), cells were not confluent near the rim (Figure 7B). In fact, the morphology of A549 cells changes from a rounded shape in confluent regions to an elongated morphology of a migrating cell in these regions. An elongated shape indicates less healthy cells, which may be due to insufficient Matrigel coating on the fibers at the edges. We did not observe significant differences in cell morphology between the negative control and any of the MALI conditions in Figure 5, including dynamic stretch conditions. Bronchial epithelial 16HBE14o− cells also adhered to the surface of the membrane, again some regions of the membrane were not covered by the cells likely due to non-uniform coating of Matrigel (Figure S9).

5. Discussion

Despite significant efforts, lung-on-a-chip devices which include perfusion and cyclic cell-stretch such as that reported in the ground-breaking work of Hu *et al.* (Huh et al., 2010) are not widely used, partially due to technical challenges associated with microfluidic systems such as clogging of fluidic channels and aerosol delivery via micro-scale air channels (Ehrmann et al., 2020). Therefore, a milli-scale lung bioreactor "MALI", where cells are cultured under air-liquid interface (ALI)

conditions with perfusion of media, cyclic cell-stretch and dose-controlled aerosolized drug delivery was developed as an alternative, to facilitate a more wide-spread use of advanced biomimetic lung models. In this study the key engineered elements of the MALI system were tested and evaluated. Firstly, a key element of the MALI system is dose-controlled delivery, based on a vibrating mesh nebulizer, which is widely used in clinical settings (Aeroneb Pro). Typically, the fraction of invested substance deposited on the cell layer can vary significantly between 0.1% to ca. 20% depending on the experimental setup and chosen deposition mechanism (Desantes et al., 2006; Paur et al., 2011). For testing of experimental drugs deposition efficiencies of less than 10% are often prohibitive due to high substance cost. The setup presented here is a dose-optimized version of the previously described ALICE Cloud technology (commercially available as VITROCELL®Cloud, VITROCELL Systems, Germany), which leverages cloud dynamics for uniform deposition of aerosols onto cells (Lenz et al., 2014; Röhm et al., 2017). The change in design reported here increases the deposition efficiency from 2.8 % per 6-well transwell insert in the ALICE Cloud to 51.5% of the invested drug onto the cells in a spatially uniform and highly reproducible way, which is a significant improvement over the traditional Cloud technology. The MALI aerosol unit described here has recently become commercially available as VITROCELL® Cloud MAX technology (VITROCELL Systems, Waldkrich, Germany), for use with standard transwell inserts in static cell culture systems. Aerosol deposition in the MALI occurs within ca. 1 min and is performed under static conditions, i.e. it is decoupled from cyclic stretch. This mimics aerosol therapy under clinical conditions where patients inhale therapeutic aerosols with a single breath followed by a ca. 1 min breath-hold period for enhanced aerosol deposition. For applications requiring long-term aerosol delivery, the nebulizer could be activated periodically during the cyclic stretch experiment, but this mode of operation was not investigated here.

Modelling the complex dynamic motion of the highly dense cloud of aerosol in the apical chamber of the MALI bioreactor is not a simple task, since the cloud density is high enough to induce multi-phase coupling. Nonetheless, the Eulerian Multiphase FEM model predicted the experimentally determined cell-delivered aerosol dose reasonably well. Empirical data show that the aerosol is relatively uniformly deposited on the cells with a dose variability of about 20% about the mean dose (for cellular resolution; Figure 4B) and a narrow annular region near the walls for the bioreactor with steeply decreasing dose. Both of these aspects are captured by the FEM model (Figure 2C). Moreover, FEM model predicted an aerosol deposition efficiency of 85%, which was corrected to 74.3% to account for the fact that only 12.6% of the invested liquid remained in the nebulizer. Considering the degree of uncertainty in the initial conditions, namely spatial distribution, speed and angular direction of the cloud droplets emitted from the vibrating mesh which were assumed to be uniform, constant (2.5 m s^{-1}) and perpendicular to the plane of the vibrating mesh, respectively (all values are approximations), the FEM model is in reasonably good agreement with the empirically determined cell-delivered dose of 51.5%. Thus, the model can be used to guide further optimization of the aerosol delivery efficiency.

The MALI bioreactor was purposely designed to be modular, housing both purposely designed and commercial membranes. Indeed, one of the most crucial elements of any stretching *in vitro* model of the lung is the membrane for cell seeding and growth, which should be elastic, stretchable, resilient to long-term cyclic strain under aqueous conditions and porous/permeable to allow for air-liquid interface culture conditions. Mechanical tests showed that the electrospun Bionate® is a suitable material with respect to its mechanoelastic properties revealing no degradation or hysteresis in the uniaxial stress-strain curve for up to 24h cyclic stretch (up to 15 % uniaxial strain, 0.2 Hz). It also has a porous structure and a high surface area to volume ratio, mimicking natural extracellular matrix in native tissues. As an important feature of quality control

during experiments, the MALI system allows for real-time monitoring of the stretch level and frequency by monitoring the pressure change in the medium reservoir and relating it to a corresponding linear strain.

The membrane also has to be conducive to cell growth which implies wettability, biocompatibility and good cell adhesion. Here, the alveolar lung epithelium cell line A549 and bronchial epithelial cell line 16HBE14o were used for basic biologic validation experiments of the MALI bioreactor system. Advanced cell culture models such as co-cultures or (immortalized) primary lung epithelial cells (hAELVi) (Kuehn, 2016), are planned for future investigations.

Cell growth and cytotoxicity assays showed that alveolar lung epithelial cells (A549) form a viable cell layer within 7 days and 3h of physiologic cyclic stretch (5% linear strain, 0.2 Hz) did not impair cell viability or morphology. These results are consistent with previous stretch studies with A549 cells and other lung epithelial cells (DiPaolo et al., 2010; McAdams et al., 2006; Tschumperlin and Margulies, 1998; Vlahakis et al., 1999). However, the hydrophobic membrane has to be pre-treated with ethanol and water to render it wettable and then coated with Matrigel to allow for sufficient growth of A549 alveolar epithelial cells. It is also noteworthy that the cells penetrate into the porous structure, which is much thicker than the basal lamina (typically less than 1 µm). Thus, the cells assemble along multiple layers within the structure instead of forming a single epithelial stratum on top of the membrane. The thickness of the membrane may also interfere with transbarrier transport processes. Besides improving the uniformity of the coating, other biocompatible materials such as natural/artificial hybrid composites with similar elastic properties but more conducive to cell growth and more effective at ensuring the formation of a contiguous cell monolayer or 3D full thickness epithelial tissue could be developed (Doryab et al., 2019). In this direction, we have recently fabricated a biohybrid membrane with mechancial properties suitable for use in stretching experiments in MALI under both physiologic and pathological

conditions (Doryab et al., 2020).

6. Conclusion

The MALI bioreactor system represents a novel dynamic *in vitro* stretch model of the alveolar air-blood interface with aerosol delivery. It combines physiologic air-liquid interface culture conditions with medium perfusion and cyclic cell-stretch mimicking blood circulation and breathing activity of the lung, respectively. The MALI system provides uniform aerosol distribution on the cells and extremely high dose efficiency (51.5%) making it suitable for testing of even costly substances such as experimental drug candidates. Finally, in consistency with previous cell stretch studies, lung epithelial cell morphology, growth and cytotoxicity were not affected by physiological strains.

Acknowledgements

We would like to thank Sezer Orak for performing the nebulization and imaging of the aerosol deposition profile in the bioreactor using the IVIS. The study was partly funded by LAV (Italian anti-vivisection league) through a fellowship to RN. The funders had no role in study design, data collection and analysis, decision to publish, or preparation of the manuscript.

References

Artzy-Schnirman A, Hobi N, Schneider-Daum N, Guenat OT, Lehr C-M, Sznitman J. 2019. Advanced in vitro lung-on-chip platforms for inhalation assays: From prospect to pipeline. *Eur. J. Pharm. Biopharm.* **144**:11–17. https://doi.org/10.1016/j.ejpb.2019.09.006.

Barapatre N, Symvoulidis P, Möller W, Prade F, Deliolanis NC, Hertel S, Winter G, Yildirim AÖ, Stoeger T, Eickelberg O, Ntziachristos V, Schmid O. 2015. Quantitative detection of drug dose and spatial distribution in the lung revealed by Cryoslicing Imaging. *J. Pharm. Biomed. Anal.* **102**:129–136.

Bélanger MC, Marois Y, Roy R, Mehri Y, Wagner E, Zhang Z, King MW, Yang M, Hahn C, Guidoin R. 2000. Selection of a polyurethane membrane for the manufacture of ventricles for a totally implantable artificial heart: Blood compatibility and biocompatibility studies. *Artif. Organs* **24**:879–888.

Bitterle E, Karg E, Schroeppel A, Kreyling WG, Tippe A, Ferron GA, Schmid O, Heyder J, Maier KL, Hofer T. 2006. Dose-controlled exposure of A549 epithelial cells at the air-liquid interface to airborne ultrafine carbonaceous particles. *Chemosphere* **65**:1784–1790.

Broßell D, Tröller S, Dziurowitz N, Plitzko S, Linsel G, Asbach C, Azong-Wara N, Fissan H, Schmidt-Ott A. 2013. A thermal precipitator for the deposition of airborne nanoparticles onto living cells-Rationale and development. *J. Aerosol Sci.* **63**:75–86. http://dx.doi.org/10.1016/j.jaerosci.2013.04.012.

Campillo N, Jorba I, Schaedel L, Casals B, Gozal D, Farré R, Almendros I, Navajas D. 2016. A Novel Chip for Cyclic Stretch and Intermittent Hypoxia Cell Exposures Mimicking Obstructive Sleep Apnea. *Front. Physiol.* **7**:1–12. http://journal.frontiersin.org/Article/10.3389/fphys.2016.00319/abstract.

Cavanaugh KJ, Cohen TS, Margulies SS. 2006. Stretch increases alveolar epithelial permeability to uncharged micromolecules. *Am. J. Physiol. Physiol.* **290**:C1179–C1188. https://linkinghub.elsevier.com/retrieve/pii/S0891584908005881.

Choe MM, Sporn PHS, Swartz MA. 2006. Extracellular Matrix Remodeling by Dynamic Strain in a Three-Dimensional Tissue-Engineered Human Airway Wall Model. *Am. J. Respir. Cell Mol. Biol.* **35**:306–313. http://www.atsjournals.org/doi/abs/10.1165/rcmb.2005-0443OC.

Darquenne C, Fleming JS, Katz I, Martin AR, Schroeter J, Usmani OS, Venegas J, Schmid O. 2016. Bridging the Gap Between Science and Clinical Efficacy: Physiology, Imaging, and Modeling of Aerosols in the Lung. *J. Aerosol Med. Pulm. Drug Deliv.* **29**:107–126. http://online.liebertpub.com/doi/10.1089/jamp.2015.1270.

Desantes JM, Margot X, Gil A, Fuentes E. 2006. Computational study on the deposition of ultrafine particles from Diesel exhaust aerosol. *J. Aerosol Sci.* **37**:1750–1769.

DiPaolo BC, Lenormand G, Fredberg JJ, Margulies SS. 2010. Stretch magnitude and frequency-dependent actin cytoskeleton remodeling in alveolar epithelia. *Am. J. Physiol. Physiol.* **299**:C345–C353. http://www.physiology.org/doi/10.1152/ajpcell.00379.2009.

Doryab A, Amoabediny G, Salehi-Najafabadi A. 2016. Advances in pulmonary therapy and drug development: Lung tissue engineering to lung-on-a-chip. *Biotechnol. Adv.* **34**:588–596. http://linkinghub.elsevier.com/retrieve/pii/S0734975016300131.

Doryab A, Tas S, Taskin MB, Yang L, Hilgendorff A, Groll J, Wagner DE, Schmid O. 2019. Evolution of Bioengineered Lung Models: Recent Advances and Challenges in Tissue Mimicry for Studying the Role of Mechanical Forces in Cell Biology. *Adv. Funct. Mater.* **29**:1903114. https://onlinelibrary.wiley.com/doi/abs/10.1002/adfm.201903114.

Doryab A, Taskin MB, Stahlhut P, Schroeppel A, Wagner DE, Groll J, Schmid O. 2020. A Biomimetic, Copolymeric Membrane for Cell-Stretch Experiments with Pulmonary Epithelial Cells at the Air-Liquid Interface. *Adv. Funct. Mater.* **Accepted**.

Ehrmann S, Schmid O, Darquenne C, Rothen-Rutishauser B, Sznitman J, Yang L, Barosova H, Vecellio L, Mitchell J, Heuze-Vourc'h N. 2020. Innovative preclinical models for pulmonary drug delivery research. *Expert Opin. Drug Deliv.*:1–16. https://www.tandfonline.com/doi/full/10.1080/17425247.2020.1730807.

Giusti S, Pagliari F, Vozzi F, Tirella A, Mazzei D, Cabiati M, Del Ry S, Ahluwalia A. 2013. SQPR 3.0: A sensorized bioreactor for modulating cardiac phenotype. In: . *Procedia Eng.*, Vol. 59, pp. 219–225.

Hänninen O, Brüske-Hohlfeld I, Loh M, Stoeger T, Kreyling W, Schmid O, Peters A. 2010. Occupational and consumer risk estimates for nanoparticles emitted by laser printers. *J.*

Nanoparticle Res. **12**:91–99.

Hein S, Bur M, Kolb T, Muellinger B, Schaefer UF, Lehr CM. 2010. The Pharmaceutical Aerosol Deposition Device on Cell Cultures (PADDOCC) in vitro system: Design and experimental protocol. *ATLA Altern. to Lab. Anim.* **38**:285–295.

Huh D, Matthews BD, Mammoto A, Montoya-Zavala M, Hsin HY, Ingber DE. 2010. Reconstituting Organ-Level Lung Functions on a Chip. *Science (80-.).* **328**:1662–1668. https://www.sciencemag.org/lookup/doi/10.1126/science.1188302.

Khan I, Smith N, Jones E, Finch DS, Cameron RE. 2005. Analysis and evaluation of a biomedical polycarbonate urethane tested in an in vitro study and an ovine arthroplasty model. Part I: Materials selection and evaluation. *Biomaterials* **26**:621–631.

Kreyling WG, Semmler-Behnke M, Takenaka S, Möller W. 2013. Differences in the Biokinetics of Inhaled Nano- versus Micrometer-Sized Particles. *Acc. Chem. Res.* **46**:714–722. http://pubs.acs.org/doi/abs/10.1021/ar300043r.

Kuehn A. 2016. Human alveolar epithelial cells expressing tight junctions to model the air-blood barrier. *ALTEX*. http://www.altex.ch/All-issues/Issue.50.html?iid=158&aid=5.

Lehmann AD, Daum N, Bur M, Lehr C-M, Gehr P, Rothen-Rutishauser BM. 2011a. An in vitro triple cell co-culture model with primary cells mimicking the human alveolar epithelial barrier. *Eur. J. Pharm. Biopharm.* **77**:398–406.

Lehmann AD, Daum N, Bur M, Lehr CM, Gehr P, Rothen-Rutishauser BM. 2011b. An in vitro triple cell co-culture model with primary cells mimicking the human alveolar epithelial barrier. *Eur. J. Pharm. Biopharm.* **77**:398–406.

Lenz A-G, Karg E, Brendel E, Hinze-Heyn H, Maier KL, Eickelberg O, Stoeger T, Schmid O. 2013. Inflammatory and Oxidative Stress Responses of an Alveolar Epithelial Cell Line to Airborne Zinc Oxide Nanoparticles at the Air-Liquid Interface: A Comparison with Conventional, Submerged Cell-Culture Conditions. *Biomed Res. Int.* **2013**:1–12. http://www.hindawi.com/journals/bmri/2013/652632/.

Lenz A-G, Stoeger T, Cei D, Schmidmeir M, Semren N, Burgstaller G, Lentner B, Eickelberg O, Meiners S, Schmid O. 2014. Efficient Bioactive Delivery of Aerosolized Drugs to Human

Pulmonary Epithelial Cells Cultured in Air–Liquid Interface Conditions. *Am. J. Respir. Cell Mol. Biol.* **51**:526–535. http://www.atsjournals.org/doi/abs/10.1165/rcmb.2013-0479OC.

Lenz A, Karg E, Lentner B, Dittrich V, Brandenberger C, Rothen-Rutishauser B, Schulz H, Ferron GA, Schmid O. 2009. A dose-controlled system for air-liquid interface cell exposure and application to zinc oxide nanoparticles. *Part. Fibre Toxicol.* **6**:32. http://particleandfibretoxicology.biomedcentral.com/articles/10.1186/1743-8977-6-32.

Mazzei D, Guzzardi MA, Giusti S, Ahluwalia A. 2010. A low shear stress modular bioreactor for connected cell culture under high flow rates. *Biotechnol. Bioeng.* **106**:n/a-n/a.

McAdams RM, Mustafa SB, Shenberger JS, Dixon PS, Henson BM, DiGeronimo RJ. 2006. Cyclic stretch attenuates effects of hyperoxia on cell proliferation and viability in human alveolar epithelial cells. *Am. J. Physiol. Cell. Mol. Physiol.* **291**:L166–L174. https://www.physiology.org/doi/10.1152/ajplung.00160.2005.

Miller C, George S, Niklason L. 2010. Developing a tissue-engineered model of the human bronchiole. *J. Tissue Eng. Regen. Med.* **4**:619–627. http://doi.wiley.com/10.1002/term.277.

Min KA, Talattof A, Tsume Y, Stringer KA, Yu JY, Lim DH, Rosania GR. 2013. The extracellular microenvironment explains variations in passive drug transport across different airway epithelial cell types. *Pharm. Res.* **30**:2118–2132.

Nahar K, Gupta N, Gauvin R, Absar S, Patel B, Gupta V, Khademhosseini A, Ahsan F. 2013. In vitro, in vivo and ex vivo models for studying particle deposition and drug absorption of inhaled pharmaceuticals. *Eur. J. Pharm. Sci.* **49**:805–818.

Oostingh GJ, Schmittner M, Ehart AK, Tischler U, Duschl A. 2008. A high-throughput screening method based on stably transformed human cells was used to determine the immunotoxic effects of fluoranthene and other PAHs. *Toxicol. Vitr.* **22**:1301–1310. https://linkinghub.elsevier.com/retrieve/pii/S0887233308000763.

Patel HJ. 2011. Characterization and Application of Dynamic in vitro Models of Human Airway. *All Grad. Theses Diss.*:143.

Paur H-R, Cassee FR, Teeguarden J, Fissan H, Diabate S, Aufderheide M, Kreyling WG, Hänninen O, Kasper G, Riediker M, Rothen-Rutishauser B, Schmid O. 2011. In-vitro cell exposure studies

for the assessment of nanoparticle toxicity in the lung—A dialog between aerosol science and biology. *J. Aerosol Sci.* **42**:668–692. http://linkinghub.elsevier.com/retrieve/pii/S0021850211000929.

Peters A, Wichmann HE, Tuch T, Heinrich J, Heyder J. 1997. Respiratory effects are associated with the number of ultrafine particles. *Am. J. Respir. Crit. Care Med.* **155**:1376–1383. http://www.atsjournals.org/doi/abs/10.1164/ajrccm.155.4.9105082.

Ravikrishnan KP. 2006. PHYSIOLOGIC BASIS OF RESPIRATORY DISEASE. *Shock* **26**:222.

Ren Y, Zhan Q, Hu Q, Sun B, Yang C, Wang C. 2009. Static stretch induces active morphological remodeling and functional impairment of alveolar epithelial cells. *Respiration* **78**:301–311.

Roan E, Waters CM. 2011. What do we know about mechanical strain in lung alveoli? *Am. J. Physiol. - Lung Cell. Mol. Physiol.* **301**:L625–L635. http://ajplung.physiology.org/lookup/doi/10.1152/ajplung.00105.2011.

Röhm M, Carle S, Maigler F, Flamm J, Kramer V, Mavoungou C, Schmid O, Schindowski K. 2017. A comprehensive screening platform for aerosolizable protein formulations for intranasal and pulmonary drug delivery. *Int. J. Pharm.* **532**:537–546. http://dx.doi.org/10.1016/j.ijpharm.2017.09.027.

Sakagami M. 2006. In vivo, in vitro and ex vivo models to assess pulmonary absorption and disposition of inhaled therapeutics for systemic delivery. *Adv. Drug Deliv. Rev.* **58**:1030–1060.

Savi M, Kalberer M, Lang D, Ryser M, Fierz M, Gaschen A, Rička J, Geiser M. 2008. A novel exposure system for the efficient and controlled deposition of aerosol particles onto cell cultures. *Environ. Sci. Technol.* **42**:5667–5674.

Savla U, Sporn PHS, Waters CM. 1997. Cyclic stretch of airway epithelium inhibits prostanoid synthesis. *Am. J. Physiol. Cell. Mol. Physiol.* **273**:L1013–L1019. http://www.physiology.org/doi/10.1152/ajplung.1997.273.5.L1013.

Schmekel B, Borgstrom L, Wollmer P. 1992. Exercise increases the rate of pulmonary absorption of inhaled terbutaline. *Chest* **101**:742–745.

Schmid O, Jud C, Umehara Y, Mueller D, Bucholski A, Gruber F, Denk O, Egle R, Petri-Fink A, Rothen-Rutishauser B. 2017. Biokinetics of Aerosolized Liposomal Ciclosporin A in Human

Lung Cells in Vitro Using an Air-Liquid Cell Interface Exposure System. *J. Aerosol Med. Pulm. Drug Deliv.* **30**:411–424. http://online.liebertpub.com/doi/10.1089/jamp.2016.1361.

Schmid O, Stoeger T. 2017. Corrigendum to “Surface area is the biologically most effective dose metric for acute nanoparticle toxicity in the lung” [Journal of Aerosol Science 99 (2016) 133–143](S0021850215301166)(10.1016/j.jaerosci.2015.12.006). *J. Aerosol Sci.* Pergamon. http://www.sciencedirect.com/science/article/pii/S0021850215301166?via%3Dihub.

Schreier H, Gagné L, Conary JT, Laurian G. 1998. Simulated lung transfection by nebulization of liposome cDNA complexes using a cascade impactor seeded with 2-CFSME0-cells. *J. Aerosol Med.* **11**:1–13.

Stein SW, Thiel CG. 2017. The History of Therapeutic Aerosols: A Chronological Review. *J. Aerosol Med. Pulm. Drug Deliv.* **30**:20–41.

Stucki AO, Stucki JD, Hall SRR, Felder M, Mermoud Y, Schmid RA, Geiser T, Guenat OT. 2015. A lung-on-a-chip array with an integrated bio-inspired respiration mechanism. *Lab Chip* **15**:1302–1310. http://xlink.rsc.org/?DOI=C4LC01252F.

Tomei AA, Choe MM, Swartz MA. 2008. Effects of dynamic compression on lentiviral transduction in an in vitro airway wall model. *Am. J. Physiol. Cell. Mol. Physiol.* **294**:L79–L86. https://www.physiology.org/doi/10.1152/ajplung.00062.2007.

Tschumperlin DJ, Margulies SS. 1998. Equibiaxial deformation-induced injury of alveolar epithelial cells in vitro. *Am. J. Physiol. Cell. Mol. Physiol.* **275**:L1173–L1183. http://ajplung.physiology.org/content/275/6/L1173%5Cnhttp://ajplung.physiology.org/content/ajplung/275/6/L1173.full.pdf%5Cnhttp://www.ncbi.nlm.nih.gov/pubmed/9843855.

Vlahakis NE, Schroeder M a, Limper a H, Hubmayr RD. 1999. Stretch induces cytokine release by alveolar epithelial cells in vitro. *Am. J. Physiol.* **277**:L167–L173.

Vozzi F, Mazzei D, Vinci B, Vozzi G, Sbrana T, Ricotti L, Forgione N, Ahluwalia A. 2011. A flexible bioreactor system for constructing in vitro tissue and organ models. *Biotechnol. Bioeng.* **108**:2129–2140.

Waters CM, Roan E, Navajas D. 2012. Mechanobiology in Lung Epithelial Cells: Measurements, Perturbations, and Responses. In: . *Compr. Physiol.* Hoboken, NJ, USA: John Wiley & Sons,

Inc., Vol. 33, pp. 48–56. http://linkinghub.elsevier.com/retrieve/pii/S1044579X15000358.

Zdrahala RJ, Zdrahala IJ. 1999. Biomedical Applications of Polyurethanes: A Review of Past Promises, Present Realities, and a Vibrant Future. *J. Biomater. Appl.* **14**:67–90.

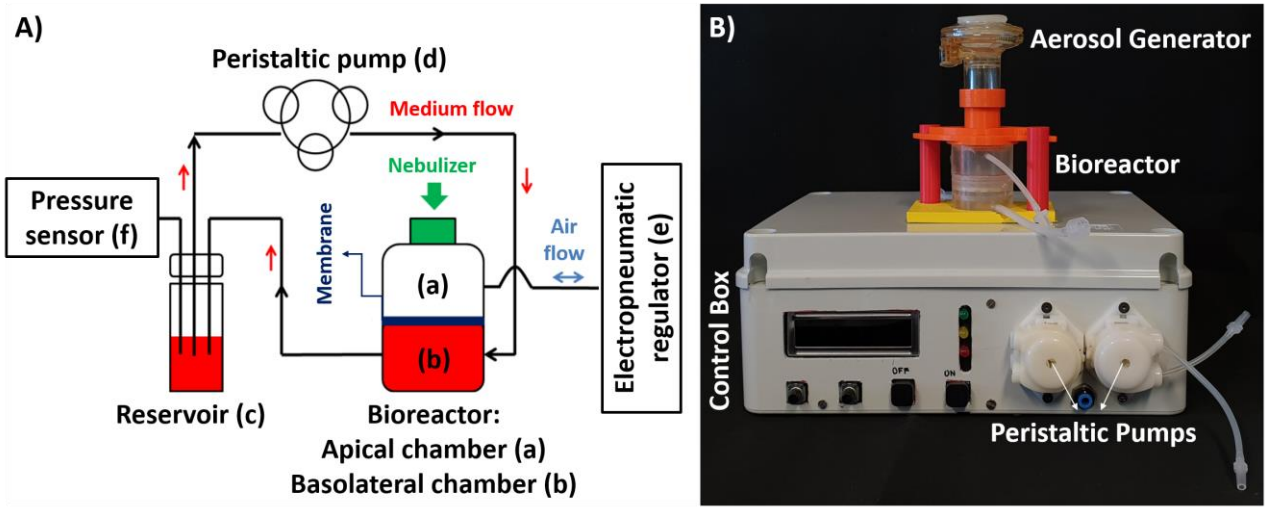

Figure 1: Setup and components of the MALI system: **A)** Schematic of the MALI system (without electronics) consisting of the bioreactor (here referred to as MALI bioreactor) with a basolateral (a) and an apical (b) chamber separated by a flexing porous membrane. The fluidic circuit for the cell culture medium comprises chamber (a), a media reservoir (c) and a pump (d). Compressed air (e) for pressure actuation of the stretchable membrane is driven through the upper circuit. A pressure sensor (f) is used to evaluate membrane deflection in real-time. The top of the bioreactor is fitted with an aerosol inlet tube for positioning of a nebulizer above the membrane. **B)** Photo of the entire MALI system.

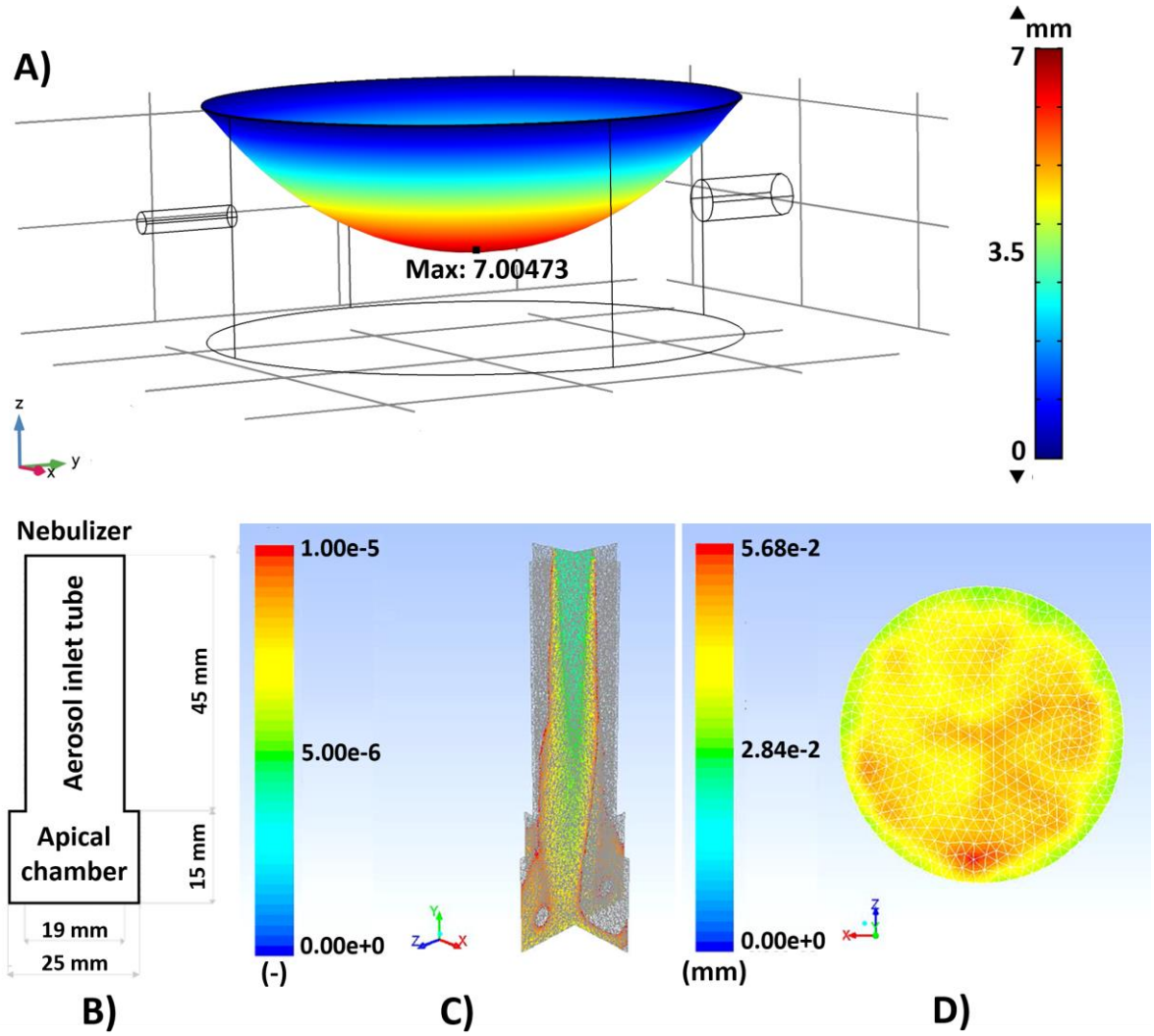

Figure 2: FEM models: A) model of the stretchable Bionate® membrane showing 3D membrane displacement surface plot for a basolateral chamber of height 14 mm with an applied apical pressure of 7 kPa. Example of CFD analysis of cloud settling: B) lateral view of the apical compartment of the bioreactor and the nebulizer tube representing the relevant domain for aerosol delivery to the membrane, which is located at the bottom of the domain. C) Volume fraction of water in aerosol cloud at 0.4 seconds after activation of the nebulizer; D) Thickness in mm and spatial distribution of deposited aerosol (liquid film) on the membrane 5 minutes after start of the nebulization.

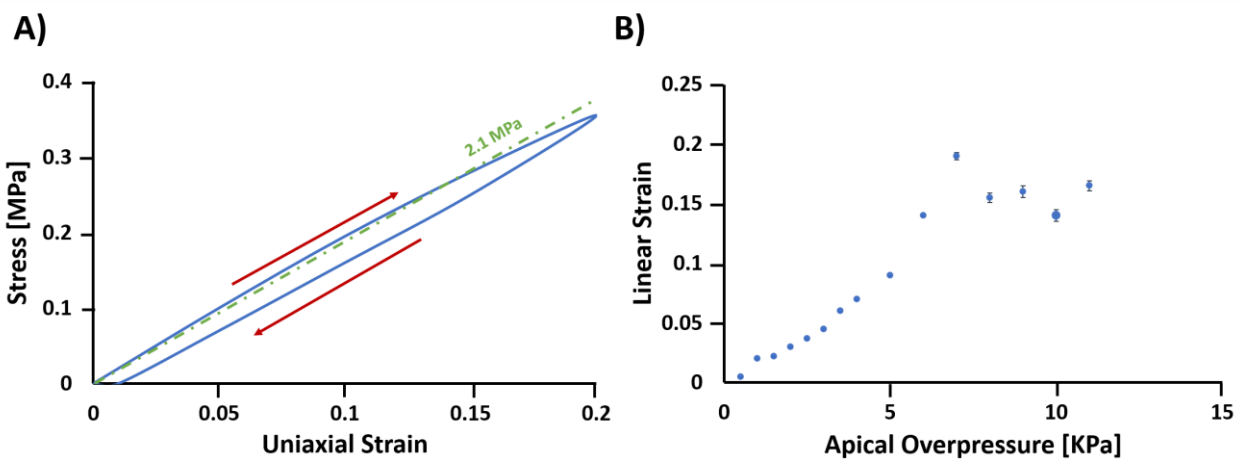

Figure 3: A) Typical uniaxial stress-strain curve of the Bionate® membrane. Red arrows indicate the direction of the test and the green dashed line is the least squares linear fit for 0 to 15% strain, giving a slope of 2.14±0.18 MPa. B) Calibration of the membrane's linear strain by the application of cyclic overpressure in the apical chamber, using the equations reported in the SI.

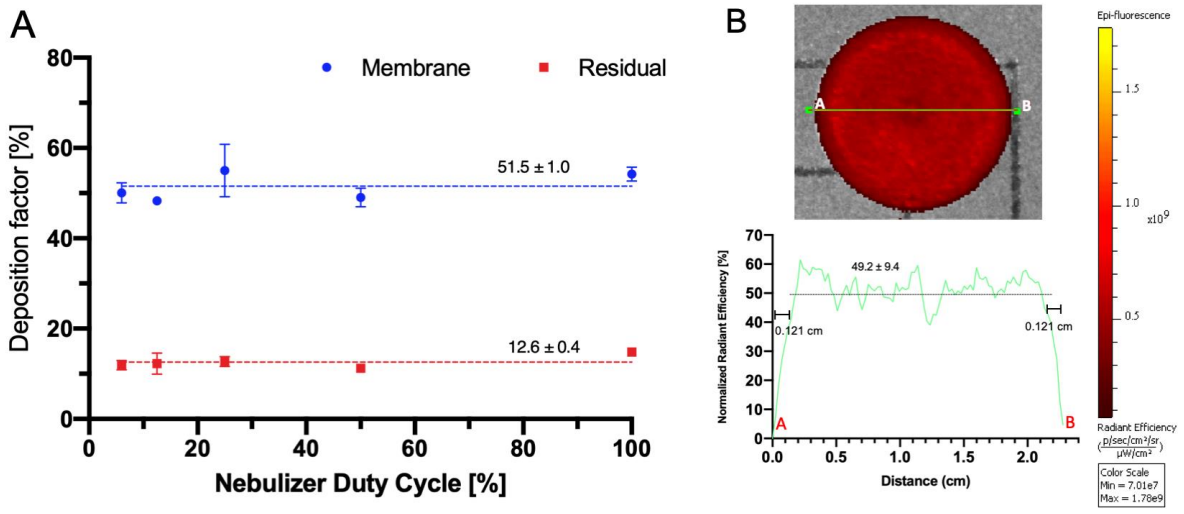

Figure 4. Aerosol delivery to the cells in the MALI system for different nebuliser duty cycles (fractional on-time of the nebulizer) is effective, reproducible and spatially uniform: **A)** Aerosol deposition (delivery) efficiency of a fluorescein salt solution was 51.5±1.0% (mean±SD; for five duty cycle settings) and a reproducibility of better than 11%.). ca. 12.6±0.4% of the administered liquid (red symbols) cannot be nebulized and remains in the nebulizer independent of duty cycle. **B)** Fluorescence intensity image of SkyBlue nanoparticles nebulised on a glass slide shows uniform delivery over the entire cell-covered area on a cellular resolution level (49.5±9.4%; pixel: 5 µm x 5 µm) except near the rim (0.121 cm), where the intensity drops sharply to zero due to the presence of the bioreactor wall.

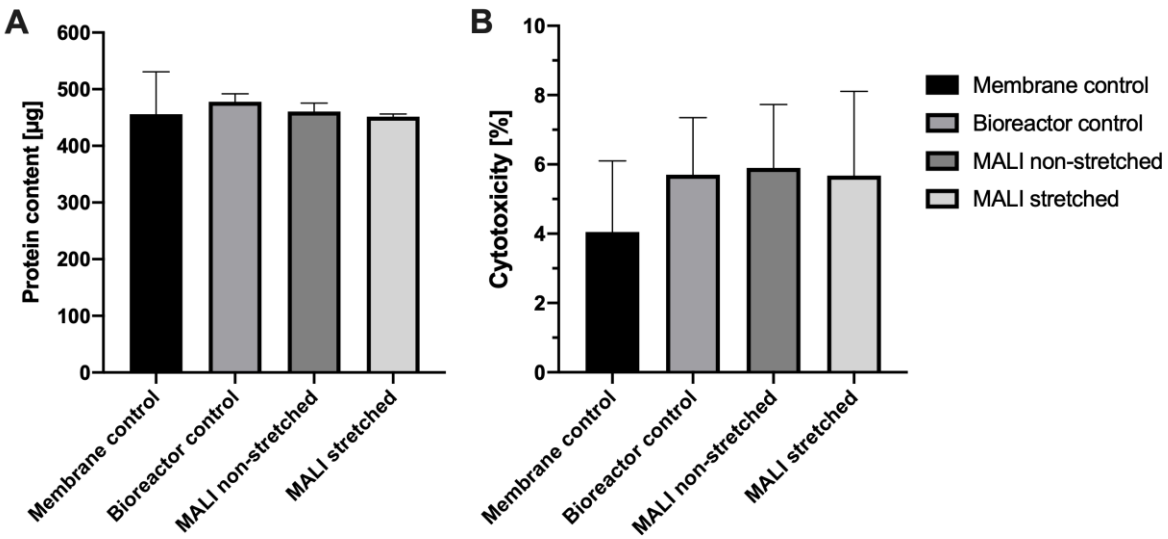

Figure 5: There are no statistically significant adverse effects on cells during handling and operation of the MALI system: A) cell growth/viability (protein content) and B) cytotoxicity (LDH release) relative to membrane control (<10% is typically considered non-cytotoxic). n=2-4; mean ± SEM.

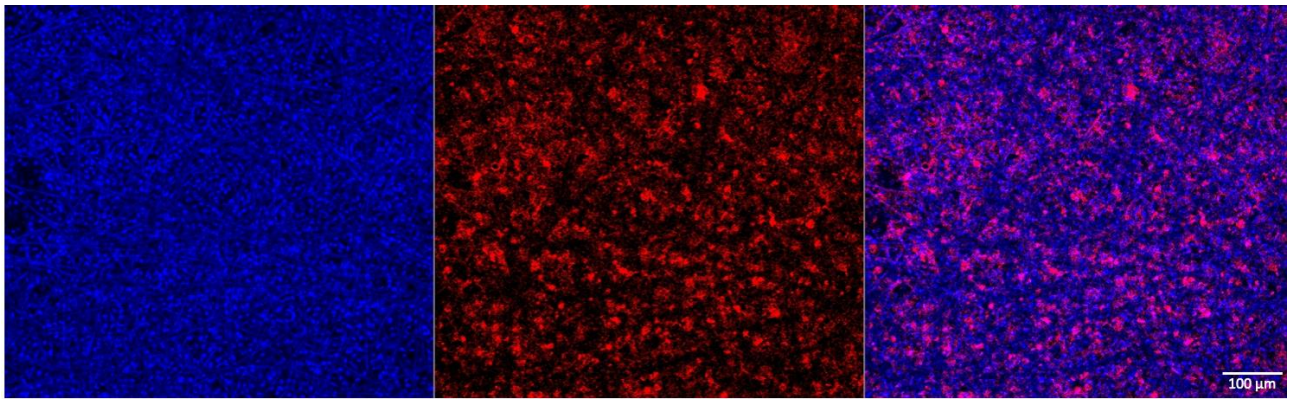

Figure 6. Confocal microscopy images showing confluent cell regions of A549 cells on Bionate® membrane (typical for all conditions) Right panel represents the cell nuclei (DAPI staining, blue); middle panel shows the actin cytoskeleton (Phalloidin staining, red); right panel presents the merged images from the left and middle panel (Scale bar: 100 µm).

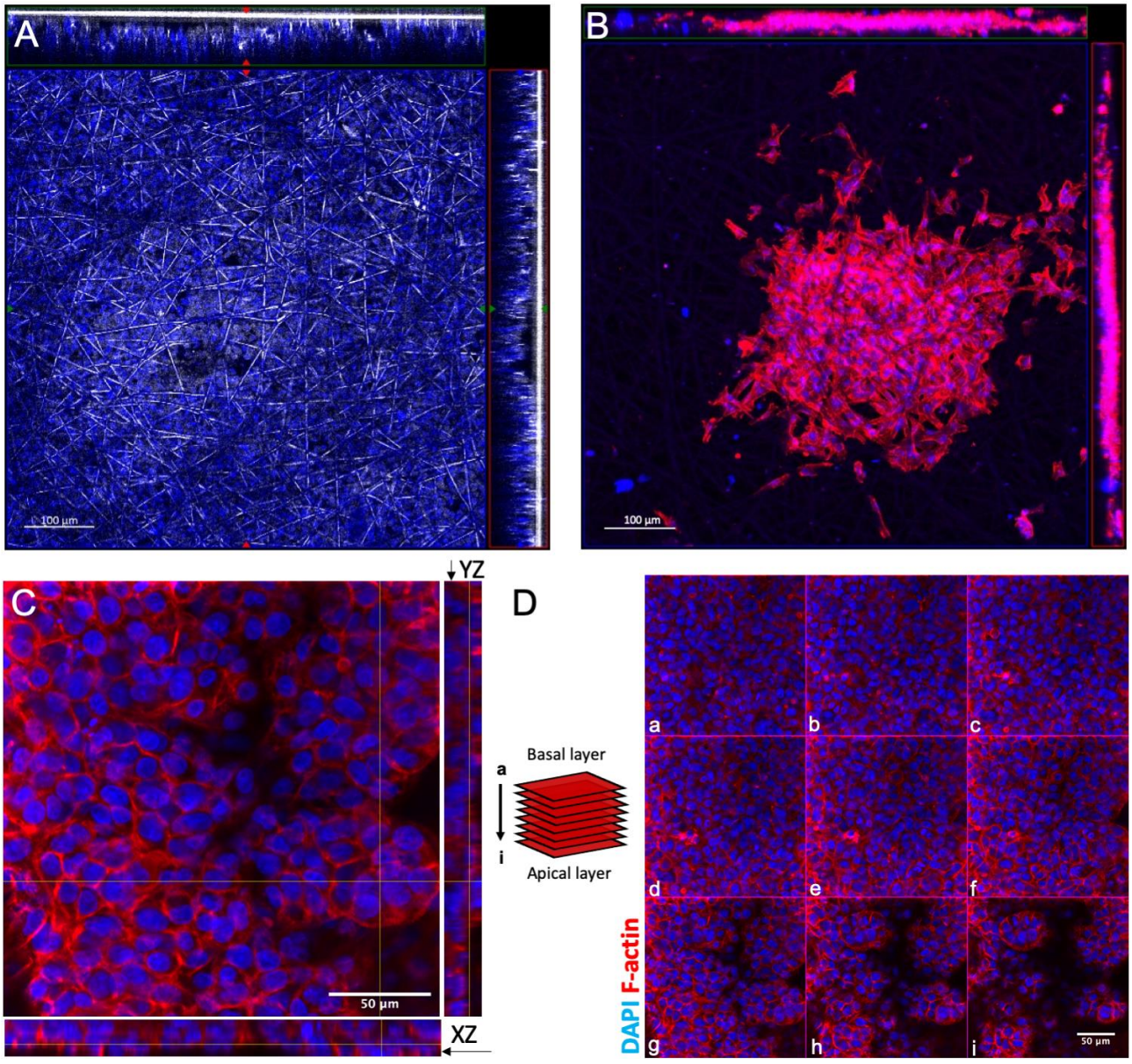

Figure 7: Confocal microscopy images showing confluent and non-confluent regions of A549 cells and their penetration into the Bionate® membrane after 3h of stretching. A) Large confluent cell region (cell nuclei are depicted in blue) embedded in the fibrous structure of the Bionate® membrane (white lines indicate fibers of membrane). From the xz- and yz- cross sections through the membrane (top and right section of the image, respectively), it is evident that the position of the cell layer within the membrane varies. It is often found near the apical side (thick white line of xz-/yz-images represent the glass cover slip on the apical side), but it can also reside within the membrane as also shown in Fig S8. (Scale bar: 100 µm) B) Non-confluent cell regions (cell nuclei in blue; cytoskeleton in red) are most prevalent near the rim of the membrane (wall of the

bioreactor). (Scale bar: 100 µm). C) Higher resolution orthogonal view of confocal microscopy images (XY) with side views of YZ (right) and XZ (bottom) (Scale bar: 50 µm) and D) confocal z-stack of A549 cells on Bionate® membrane (covering a total depth of 16 µm), showing confluent cell regions of A549 cells. Both panel C and D demonstrate that the alveolar epithelial cell layer is at least partially multi-layered rather than the mono-layered structure found in the lung. (Scale bar: 50 µm) Cell nucleus (DAPI, blue), F-actin cytoskeleton (phalloidin, red).

[i] DC and AD share first authorship; AA and OS share senior authorship.

[ii] The term "linear strain" when applied to alveolar distension refers to a change in alveolar radius as described in the SI, section H.